Available online at www.sciencedirect.com
SCIENCE DIRECT
Polymer 47 (2006) 5187–5195
polymer
www.elsevier.com/locate/polymer

A molecular thermodynamic model for binary lattice polymer solutions

Jianyong Yang, Qiliang Yan, Honglai Liu *, Ying Hu

Department of Chemistry and Lab for Advanced Materials, East China University of Science and Technology, Shanghai 200237, China

Received 4 November 2005; received in revised form 28 April 2006; accepted 7 May 2006
Available online 30 May 2006

Abstract

A molecular thermodynamic model for binary lattice polymer solutions with concise and accurate expressions for the Helmholtz energy of mixing and other thermodynamic properties is established. Computer simulation results are combined with the statistical mechanics to obtain the expressions. Yan et al.'s model for Ising lattice and the sticky-point model of Cumming, Zhou and Stell are incorporated in the derivation. Besides the nearest neighbor cavity correlation function obtained from the Ising lattice, the long range correlations beyond the close contact pairs are represented by a parameter λ, the linear chain-length dependence of which is obtained by fitting the simulated critical parameters of two systems with chain lengths of 4 and 200. The predicted critical temperatures and critical compositions, spinodals and coexistence curves as well as internal energies of mixing for systems with various chain lengths are in satisfactory agreement in comparison with the computer simulation results and experimental data indicating the superiority of the model over other theories. The model can serve as a basis to develop more efficient models for practical applications.

Keywords: Molecular thermodynamics; Lattice model; Binary polymer solutions

1. Introduction

A variety of polymer-solution theories have been developed during the latter half of the last century. Among them, the lattice model is still a convenient starting point for the prediction of phase equilibria of the various polymer systems. The most widely used and best known is the Flory–Huggins lattice theory [1,2] based on a mean-field approach, which illustrates in a simple way the competition between the entropy of mixing and the attractive forces that induces liquid–liquid phase separation at low temperatures with an upper critical solution temperature. However, it is known that a mean-field approximation cannot correctly describe the shape of the coexistence curves near the critical point compared with experimental data [3–5].

Although some refinements were made progressively [6,7], the lattice cluster theory developed by Freed and co-workers [8–13] in 1990s was a landmark because it is formally an exact mathematical solution of the Flory–Huggins lattice with a complete and systematic analysis. Similar to Mayer's theory for non-ideal gases, they developed a double expansion in power series with respect to the reciprocals of the coordination number z and the temperature T. However, because of the complexity of the expansion, pages of equations are involved even truncated at the first order or at the second order, the practical usage of the theory for liquid–liquid equilibria calculations is limited. Sometimes, the results are unsatisfactory, for example, the prediction of critical compositions exhibit unpleasant kink, which is in contradictory with the computer simulation results [10,14,15].

To make the Freed theory accessible for engineering purposes, Hu and co-workers [16–19] reported a revised Freed model and a double-lattice model, the latter was designed to account for the orientation effect of hydrogen bonding. The empirical parameters in their model arose from the truncation of higher order terms in the expansion of the Helmholtz energy of mixing, were determined by using a few Monte–Carlo simulation data of the system with chain length of $r_1 = 1$ and $r_2 = 100$. Lambert et al. [20] and Bae et al. [21] have made similar improvements. These models provide better description of the experimental phase behavior including those with a lower critical solution temperature, loop and hour-glass type liquid–liquid coexistence curves. Recently, Chen et al. [22,23] extended RFT to the random copolymer solutions, Bae et al. [24] extend their modified double-lattice model to polymer blend systems.

More than half a century, we have witnessed the problems we faced on the lattice models. It is difficult to obtain concise

* Corresponding author. Tel.: +86 21 64252921; fax: +86 21 64252921.
E-mail address: hlliu@ecust.edu.cn (H. Liu).

0032-3861/$ - see front matter © 2006 Elsevier Ltd. All rights reserved.
doi:10.1016/j.polymer.2006.05.009

List of symbols

A	Helmholtz function
U	internal energy
N_r	number of total sites
N	number of molecules
T	temperature
T^*	reduced temperature
g	radial distribution function
k	Boltzmann constant
z	coordination number
r	chain length
q	surface area parameter
p	pressure
w	weight fraction
M_w	molecular weight

Greek letters

λ	parameter characterizing the long-range correlations
ε	exchange energy
ε_{ij}	interaction energy of i–j pair
ϕ	volume fraction
θ	surface fraction
μ	chemical potential

and accurate analytical expressions for Helmholtz energy of mixing and other thermodynamic properties except by infinite series expansion. Even for the simplest Ising lattice, only the one-dimensional and the two-dimensional lattice can be solved completely on the basis of statistical mechanics. The three-dimensional lattice has yielded so far to rigorous analysis only by way of series expansion [25]. We have to find a way out other than the traditional statistical mechanical derivation. Introducing the molecular simulation into statistical mechanics to establish models seems to be an effective means to solve this problem. A good example is the well-known Carnahan–Starling equation for hard sphere fluids [26]. The equation was established by a linear combination of the PY pressure equation and the PY compressibility equation; coefficients of them were judged by the computer simulation results. In our previous work, we have developed an equation of state for hard-sphere chain fluids in a similar way [27]. Based on the sticky-point model of Cummings, Zhou and Stell [28–30], an expression of residual Helmholtz energy in terms of the cavity correlation function (CCF) was established where the nearest-neighbor CCF was derived from the rigorous Tildesley–Streett equation [31] inducted from computer-simulation results of hard dumbbells, the next-to-nearest neighbor CCF was obtained by fitting the simulation data of trimers. A concise equation of state similar to Carnahan–Starling equation was finally obtained for hard-sphere chain fluids.

We want to study the lattice polymer along the similar approach, i.e. combining the molecular simulation with statistical mechanics. Based on our previous work of Yan et al. [32] for Ising lattice, we will go a step further to Flory–Huggins lattice. The cavity correlation function (CCF) formalism that has been successfully used in hard-sphere chain fluids previously [27] will be adopted again. The long range correlations beyond the close contact pair are represented by a parameter λ, the linear chain-length dependence of which is obtained by fitting the critical parameters of two different systems with chain lengths of 4 and 200. A concise and accurate analytical expression for the Helmholtz energy of mixing is then obtained. The molecular thermodynamic model is then investigated comprehensively by comparing the predicted critical temperatures and compositions, coexistence curves, spinodals and the internal energies of mixing with the corresponding simulation results for different systems with various chain lengths. A few examples for practical application are also presented. Finally, concluding remarks are given.

2. The molecular thermodynamic model

2.1. The general framework

We start from a simple cubic lattice containing N_r sites with a coordination number $z=6$. The lattice is filled with N_1 solvent molecules, each one occupies one site, $r_1=1$, and N_2 chain molecules with chain length r_2. Only the nearest-neighbor interactions are considered.

To obtain the Helmholtz energy of mixing $\Delta_{mix}A$, we design a three-step process: (1) dissociate the pure chains to form pure monomers; (2) mix solvents and monomers to form a mixture; (3) associate the monomers into chain molecules. The bond energies involved in the dissociation step (1) and the association step (3) are mutual compensated, therefore, they need not be considered in this scheme. The Helmholtz energy of mixing $\Delta_{mix}A$ can be expressed as

$$\Delta_{mix}A = -T\Delta_{mix}S_0 + \Delta A_1 + \Delta A_2 + \Delta A_3 \quad (1)$$

The athermal entropy of mixing $\Delta_{mix}S_0$ is introduced because the ΔA_1, ΔA_2, ΔA_3 calculated later are the residual Helmholtz energy change.

For the athermal entropy of mixing $\Delta_{mix}S_0$, we simulated the chemical potentials and the probability of 1–1 pairs for the athermal mixtures with different r_2 using chain insertion method [33], and compared them with those calculated by the Flory–Huggins theory [1] and the Guggenheim theory [6]. A cubic lattice of $16\times16\times16$ sites with periodic boundaries in three directions was used. Molecules of component 1 were treated as cavities. Total of 10^7 configurations were generated for each state where the first 2×10^5 configurations before equilibrium were not included. The chain insertion was carried out every 10^3 steps. For each of those configurations to insert the chain, the insertion procedure was repeated several times

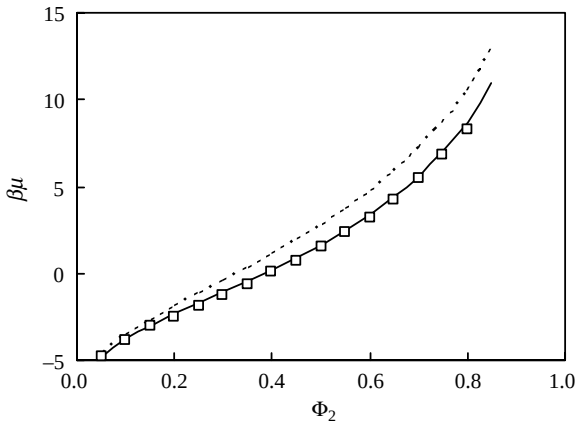

Fig. 1. Chemical potentials of an athermal mixture with $r_2=8$. Squares: MC results of this work. Dash line: predicted by Flory–Huggins theory. Solid line: predicted by Guggenheim theory.

dependent on the density. As shown in Fig. 1 for chemical potentials of an athermal mixture with $r_2=8$, and in Fig. 2 for the generalized plot of the probabilities of 1–1 pairs versus surface fraction for athermal mixtures with various chain lengths, the results from the Guggenheim's prediction are perfect, much better than that from the Flory–Huggins theory. We therefore, adopt Guggenheim's athermal entropy of mixing [6] for $\Delta_{\text{mix}}S_0$ in this work,

$$-\frac{\Delta_{\text{mix}}S_0}{N_r k}=\frac{\Delta_{\text{mix}}S_{\text{Guggenheim}}}{N_r k}$$
$$=\phi_1\ln\phi_1+\frac{\phi_2}{r_2}\ln\phi_2$$
$$+\frac{z}{2}\left[\phi_1\ln\frac{\theta_1}{\phi_1}+\phi_2\frac{q_2}{r_2}\ln\frac{\theta_2}{\phi_2}\right] \quad (2)$$

Here, ϕ_i and θ_i are the volume fraction and surface fraction of component i, respectively, calculated by

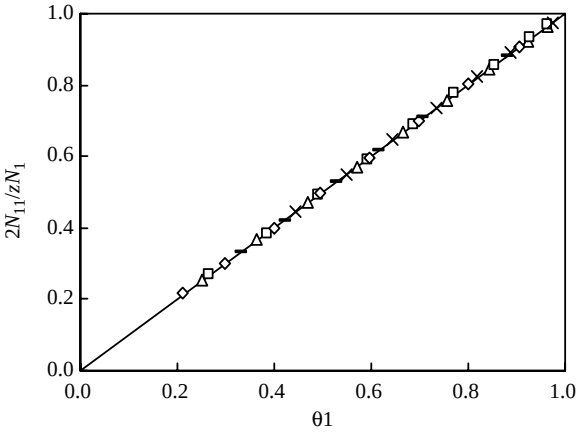

Fig. 2. Probabilities of 1–1 pairs of athermal mixtures with different chain lengths MC results of this work: $r_2=4$ (open triangles); $r_2=8$ (open diamonds); $r_2=16$ (open squares); $r_2=32$ (short bars); $r_2=64$ (crosses). Solid line: predicted by Guggenheim theory.

$$\phi_i=\frac{N_i r_i}{N_1 r_1+N_2 r_2},\quad \theta_i=\frac{N_i q_i}{N_1 q_1+N_2 q_2} \quad (3)$$

where q_i is the surface area parameter defined as

$$zq_i=r_i(z-2)+2 \quad (4)$$

For the step (1) and step (3), the formalism of chemical association through the cavity correlation function y in our previous work [27] based on the sticky-point model of Cummings, Zhou and Stell [28–30] can be employed. The r-particle cavity correlation function (CCF) $y^{(r_2)}$ is defined by

$$y^{(r_2)}=\exp(\beta\varepsilon^{(r_2)})g^{(r_2)} \quad (5)$$

where $g^{(r_2)}$ is the r-particle correlation function, $\varepsilon^{(r_2)}$ is the attractive energy of a chain, $\beta=1/kT$. The expression of Helmholtz energy of association has been derived as [27],

$$\beta[A(\alpha)-A(\alpha=0)]=-\frac{N_2}{r_2}\left(\alpha-\int_{\alpha=0}^{\alpha=\alpha}\alpha\mathrm{d}\ln y^{(r_2)}\right) \quad (6)$$

where α is the degree of association. Differentiate the Helmholtz energy with respect to density; we obtain the equation of state. Integrate again; we then have the residual Helmholtz energy A^{r},

$$\beta[A^{\text{r}}(\alpha=1)-A^{\text{r}}(\alpha=0)]=-N_2\ln y^{(r_2)}$$
$$=-N_2\ln g^{(r_2)}-N_2\beta\varepsilon^{(r_2)} \quad (7)$$

For the first dissociation step, it is the reverse of an association. For a pure lattice polymer, when it dissociates into close-packed monomers, $g^{(r_2)}=1$. From Eq. (7) we then have,

$$\Delta A_1=N_2\varepsilon^{(r_2)} \quad (8)$$

For the third step, associate monomers into chains, we have from Eq. (7),

$$\Delta A_3=-kTN_2\ln y^{(r_2)}=-kTN_2\ln g^{(r_2)}-N_2\varepsilon^{(r_2)} \quad (9)$$

Obviously, $N_2\varepsilon^{(r_2)}$ Eq. (8) and Eq. (9) cancels, only a term with $g^{(r_2)}$ is remained.

For the second step, ΔA_2 is the residual Helmoltz energy of mixing of an Ising lattice. Here we use directly Yan et al.'s result [32]. It is expressed effectively by a truncated polynomial,

$$\Delta A_2=\Delta_{\text{mix}}A^{\text{r}}_{\text{Ising}}$$
$$=N_r kT\left[\frac{z}{2T^*}\phi_1\phi_2-\frac{z}{4T^*}\phi_1^2\phi_2^2-\frac{z}{12T^{*3}}\phi_1^2\phi_2^2\left(\phi_1^2+\phi_2^2\right)\right] \quad (10)$$

where $T^*=kT/\varepsilon$ is a reduced temperature, $\varepsilon=\varepsilon_{11}+\varepsilon_{22}-2\varepsilon_{12}$ is the exchange energy between solvents 1 and monomers 2, ε_{ij} is the attractive energy of i–j pair.

Eq. (l) now becomes.

$$\Delta_{\text{mix}}A=-T\Delta_{\text{mix}}S_{\text{Guggenheim}}+\Delta_{\text{mix}}A^{\text{r}}_{\text{Ising}}-kTN_2\ln g^{(r_2)} \quad (11)$$

All the procedures to calculate the Helmholtz energy of mixing are now focused on the r-particle correlation function $g^{(r_2)}$.

2.2. The r-particle correlation function

At present, it is almost impossible to derive an explicit expression for $g^{(r_2)}$ solely by statistical mechanics. Zhou and Stell [30] adopted a linear approximation and simplified the r-particle cavity correlation function by using the nearest-neighbor two-particle CCF raised to an empirical power. In our previous work for the hard-sphere chain fluids [27], we used the next to nearest correlations, which were determined by simulation. In this work, we follow the similar measure. If we adopt Kirkwood's superposition approximation, we can write $g^{(r_2)} = (g^{(2)})^{r_2-1}$ where $g^{(2)}$ is the radial distribution function. However, this approximation neglects the long-range correlations. We then introduce a parameter λ into the exponential to account for the long range correlations beyond the close contact pair, we write

$$g^{(r_2)} = (g^{(2)})^{r_2-1+\lambda} \tag{12}$$

where $g^{(2)}$ and λ are to be determined. The feasibility of the Eq. (12) with λ included is to be identified.

The radial distribution function $g^{(2)}$ in the above equation is that of an Ising lattice. In our previous work [32], we have derived expressions for the local volume fractions ϕ_{22} and ϕ_{11} through the non-randomness factor,

$$\frac{\phi_{22}}{\phi_{21}} = \frac{\phi_2}{\phi_1}\left(\phi_2 + \phi_1 \exp\left(\frac{1}{T^*}\right)\right) \tag{13}$$

Correspondingly, we can write the radial distribution function as

$$g^{(2)} = \frac{\phi_{22}}{\phi_2} = \frac{1 + \phi_1(\exp(1/T^*) - 1)}{1 + \phi_1\phi_2(\exp(1/T^*) - 1)} \tag{14}$$

Combine Eqs. (2), (10), (12) and (14) with Eq. (11), we have a concise form of the Helmholtz energy of mixing for the lattice chain fluids, which is composed of three terms: the Guggenheim's athermal entropy of mixing, the Helmoltz energy of mixing of an Ising lattice, and the contribution of dissociation and association expressed by the r-particle correlation function, where includes a parameter λ characterizing the long-range correlations beyond the close contact pairs. The equation reads

$$\begin{aligned}\frac{\Delta_{\mathrm{mix}}A}{N_{\mathrm{r}}kT} &= -\frac{\Delta_{\mathrm{mix}}S_{\mathrm{Guggenheim}}}{N_{\mathrm{r}}k} + \frac{\Delta_{\mathrm{mix}}A^{\mathrm{r}}_{\mathrm{Ising}}}{N_{\mathrm{r}}kT} - \frac{N_2 \ln g^{(r_2)}}{N_{\mathrm{r}}} \\ &= \phi_1 \ln \phi_1 + \frac{\phi_2}{r_2}\ln \phi_2 \\ &\quad + \frac{z}{2}\left[\phi_1 \ln\frac{\theta_1}{\phi_1} + \phi_2\frac{q_2}{r_2}\ln\frac{\theta_2}{\phi_2}\right] + \frac{z}{2T^*}\phi_1\phi_2 \\ &\quad - \frac{z}{4T^{*2}}\phi_1^2\phi_2^2 - \frac{z}{12T^{*3}}\phi_1^2\phi_2^2(\phi_1^2 + \phi_2^2) \\ &\quad - \frac{r_2 - 1 + \lambda}{r_2}\phi_2 \ln\left(\frac{1 + \phi_1(\exp(1/T^*) - 1)}{1 + \phi_1\phi_2(\exp(1/T^*) - 1)}\right)\end{aligned} \tag{15}$$

If $r_2 = 1$, Eq. (15) returns to Eq. (10) of the Ising lattice. Using the well-known Gibbs–Helmholtz equation, differentiate Eq. (15) with respect to $1/T^*$, we have the internal energy of mixing,

$$\begin{aligned}\frac{\Delta_{\mathrm{mix}}U}{N_{\mathrm{r}}\varepsilon} &= \frac{z}{2}\phi_1\phi_2 - \frac{z}{2T^*}\phi_1^2\phi_2^2 - \frac{z}{4T^{*2}}\phi_1^2\phi_2^2(\phi_1^2 + \phi_2^2) \\ &\quad - \frac{r_2 - 1 + \lambda}{r_2}\phi_1\phi_2 \exp(1/T^*) \\ &\quad \times \ln\left(\frac{1}{1 + \phi_1[\exp(1/T^*) - 1]} - \frac{\phi_2}{1 + \phi_1\phi_2[\exp(1/T^*) - 1]}\right)\end{aligned} \tag{16}$$

The parameter λ characterizing the long-range correlations is remained to be determined.

2.3. Phase equilibrium calculations

The chemical potential of component i can be derived through

$$\begin{aligned}\frac{\mu_1 - \mu_1^{\varnothing}}{kT} &= \left(\frac{\partial \Delta_{\mathrm{mix}}A}{\partial N_1}\right)_{T,V,N_2}, \\ \frac{\mu_2 - \mu_2^{\varnothing}}{kT} &= \left(\frac{\partial \Delta_{\mathrm{mix}}A}{\partial N_2}\right)_{T,V,N_1}\end{aligned} \tag{17}$$

Coexistence curves can be obtained by chemical-potential equalities,

$$\mu_1^{(\alpha)} = \mu_1^{(\beta)}, \qquad \mu_2^{(\alpha)} = \mu_2^{(\beta)} \tag{18}$$

Spinodal and critical point are obtained by

$$\left(\frac{\partial^2 \Delta_{\mathrm{mix}}A/N_{\mathrm{r}}kT}{\partial\phi_1^2}\right)_{T,V} = 0, \quad \left(\frac{\partial^3 \Delta_{\mathrm{mix}}A/N_{\mathrm{r}}kT}{\partial\phi_1^3}\right)_{T,V} = 0 \tag{19}$$

2.4. Parameter λ

If we neglect the long-range correlations, $\lambda = 0$, we can still use the above equations to carry out the phase equilibrium calculations. Later we will show that although the prediction is

better than that of the Flory–Huggins theory, the discrepancy is still serious. Introduction of λ is definitely necessary.

We express the chain-length dependence of λ as

$$\lambda = \frac{(r_2-1)(r_2-2)}{r_2^2}(ar_2+b) \tag{20}$$

The pre-factor is introduced because when $r_2=1$ or 2, $\lambda=0$. The main part is a linear function. To determine the parameter λ characterizing the long-range correlations, we can either use the simulation results of the critical parameters or that of the internal energies of mixing. Here we adopted the first approach. Simulated critical temperatures and compositions for two systems with chain lengths of 4 and 200 [14,15] were adopted. We obtained $a=0.1321$ and $b=0.5918$.

Now we have a complete molecular thermodynamic model for a binary lattice polymer solution as shown by Eqs. (15) and (20).

3. Comparisons with results by simulation and other theories

3.1. Critical temperatures and compositions

Figs. 3 and 4 are the chain-length dependence of the critical temperature and the critical volume fraction for binary lattice polymer solutions. Simulation results of Yan et al. [14] and Panagiotopoulos et al. [15] are adopted. As shown in the figures, the prediction of Flory–Huggins theory is poor. The prediction of this work when $\lambda=0$, i.e. neglect the long-range correlations, is improved, however, still has discrepancies. As for the Freed theory, the prediction of critical temperatures is good, as shown in Fig. 3, it is only slightly overestimated. However, unfortunately, the prediction of critical volume fractions is unexpectedly bad as shown by the unpleasant kink in Fig. 4. When the long-range correlation is incorporated in this work, by introducing a parameter λ, the prediction of the chain length dependence of the critical parameters is much improved as shown in these figures.

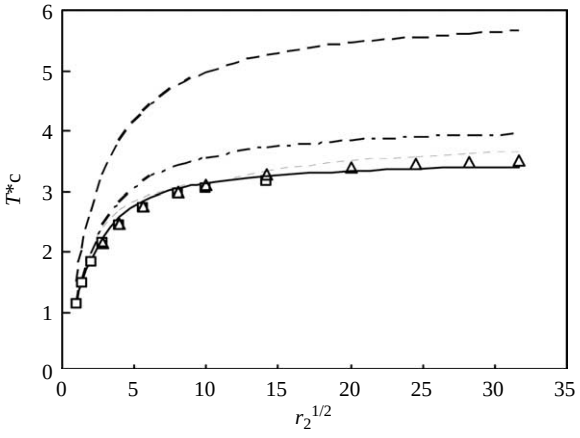

Fig. 3. Chain-length dependence of the reduced critical temperature, $T_c^* \sim r_2^{1/2}$ plot. Square: MC data of Yan et al. [14]. Triangles: MC data of Panagiotopoulos et al. [15]. Solid line: this work. Dot dash line: this work, $\lambda=0$. Dash line: Flory–Huggins's theory. Dot line: Freed theory.

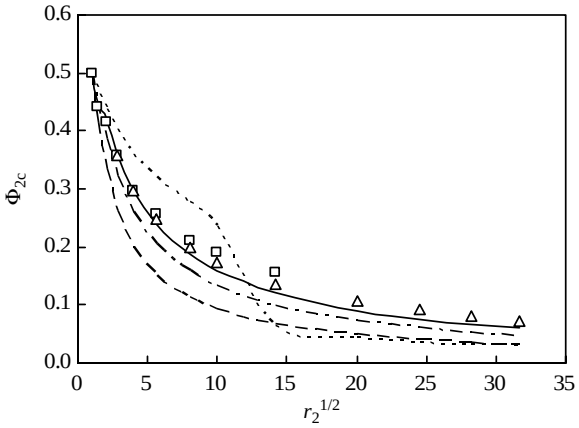

Fig. 4. Chain-length dependence of the critical volume fraction, $\phi_{2c} \sim r_2^{1/2}$ plot. Legend: the same as Fig. 3.

3.2. Coexistence curves

Figs. 5–8 show comparisons between simulated coexistence curves with those predicted by various theories for systems with $r_2=4$, 32, 100 and 400. Simulation results of Yan et al. [14] and Panagiotopoulos et al. [15] are adopted. Again, the Flory–Huggins theory gives much higher and narrower curves indicating poor predictions. Results by this work and by Freed theory are also presented. Generally, this work shows satisfactory results, slightly better than those by Freed theory.

3.3. Spinodals

Figs. 9 and 10 show comparisons between simulated spinodals with those predicted by various theories for systems with $r_2=18$ and 60. Simulation results of Rodriguez et al. [34] are adopted. The MC data of critical points are taken from Yan et al. [14]. As shown in these figures, this work gives satisfactory predictions, slightly better than that by the Freed theory, much better than that by Flory–Huggins theory.

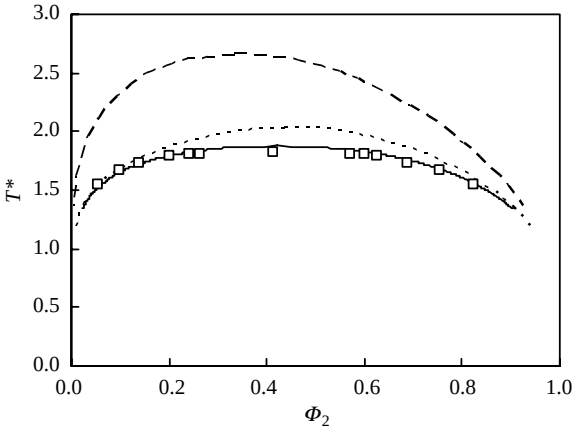

Fig. 5. Coexistence curves of a binary lattice polymer solution with $r_2=4$. Squares: MC data by Yan et al. [14]. Solid line: this work. Dash line: Flory–Huggins's theory. Dot line: Freed theory.

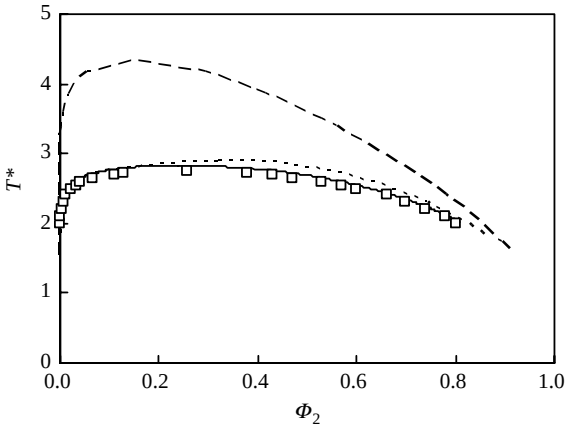

Fig. 6. Coexistence curves of a binary lattice polymer solution with $r_2=32$. Legend: the same as Fig. 5.

3.4. Internal energies of mixing

We simulated the internal energies of mixing for binary lattice polymer solutions with various chain lengths by counting the numbers of different contact segment pairs. The simulation box was a cubic lattice of $80\times80\times80$ with periodic boundaries in three directions. The Rosenbluth and Rosenbluth method [35] was adopted. The first 2×10^7 configurations before equilibrium were skipped. In the following 2.5×10^7 configurations contact segment pairs were calculated every 10^4 steps. Figs. 11 and 12 are two examples with $r_2=8$ and 64, respectively. The ordinate is a normalized internal energies of mixing expressed as $z\Delta_{mix}U/2N_r\varepsilon\phi_1\phi_2$ which is more sensible at the dilute region and the very concentrate region. Calculations of this work are performed by Eq. (16). Flory–Huggins theory predicts a constant normalized internal energy of mixing of 1.0, which cannot be verified by the simulation results as shown in the two figures. Freed theory and this work both give a good prediction at three different temperatures. Freed theory's prediction shows over-estimated results at lower temperature. Prediction of this work behaves slightly better.

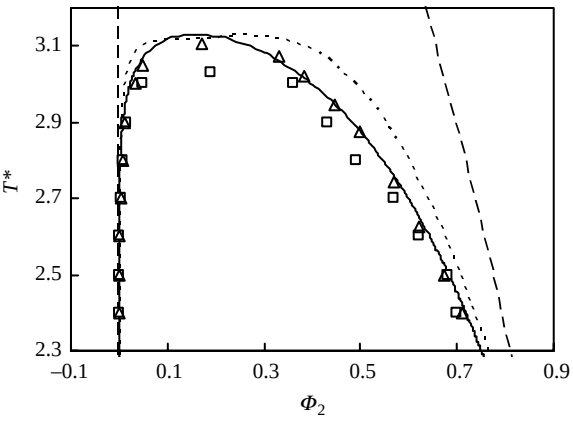

Fig. 7. Coexistence curves of a binary lattice polymer solution with $r_2=100$. Squares: MC data by Yan et al. [14]. Triangles: MC data by Panagiotopoulos et al. [15]. Solid line: this work. Dash line: Flory–Huggins's theory. Dot line: Freed theory.

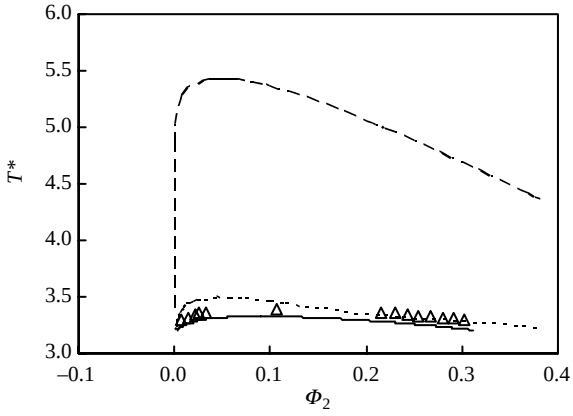

Fig. 8. Coexistence curves of a binary lattice polymer solution with $r_2=400$. Legend: the same as Fig. 7.

4. Applications to real systems

To calculate liquid–liquid equilibria of real systems, we need the model parameters r_2 and ε/k. In this work, the critical temperature is used to determine ε/k. For r_2, there are two simple choices [20,21]. One is to estimate the value of r_2/r_1 by the ratio of the molar volumes of the corresponding components at a specified temperature. The second is to obtain r_2 by fitting the critical composition. Similar to many other authors [16,20,21], we select the second choice for the first two examples. For accounting the molecular weight dependence of r_2, we adopt the direct proportional relationship between M_w and r_2 and fix ε/k as a constant for the last two cases.

Fig. 13 shows coexistence curves of poly(isobutylene)(-PIB)/diisobutyl ketone systems where the polymer has two different molecular weights, 22,700 and 285,000. Experimental data are taken from literature [36]. The results calculated by this work are presented showing good fit.

Fig. 14 shows the binodal and spinodal curves of polystyrene(PS)/methyl cyclohexane system. The molecular weight of PS is 37,900 [37]. As shown in this figure, although there is a slight deviation between the experimental data and

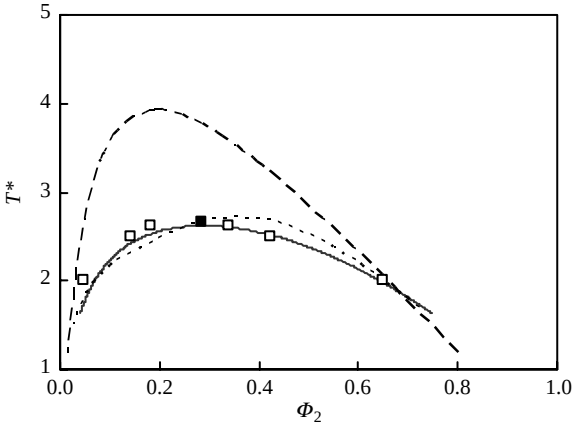

Fig. 9. Spinodal curves for a binary lattice polymer solution with $r_2=18$. Open squares: MC data by Rodriguez et al. [34]. Solid squares: critical point by Yan et al. [14]. Solid line: this work. Dash line: Flory–Huggins's theory. Dot line: Freed theory.

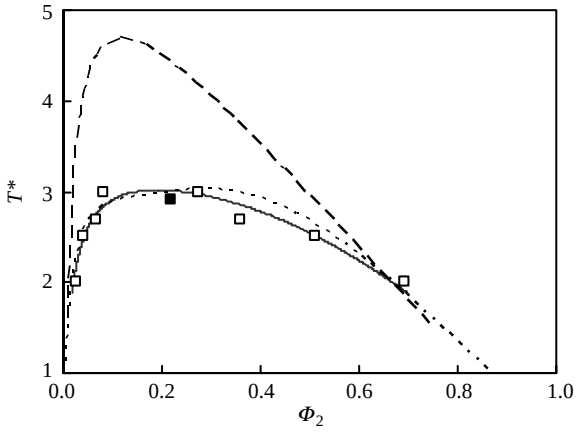

Fig. 10. Spinodal curves for a binary lattice polymer solution with $r_2=30$. Legend: the same as Fig. 9.

calculated results of the spinodal curve, our model can reproduce the experimental data well.

Fig. 15 compares calculated and experimental coexistence curves for the PS/cyclohexane mixtures where the molecular weights of PS are 20,400, 100,000 and 610,000, respectively. Experimental data are from literature [38]. In this work, we fix the values of M_w/r_2 and ε/k as constants, which are $M_w/r_2=135.7$ and $\varepsilon/k=87.1$ K. From the figure we can see that the description is good for the long-chain case, however, it gradually deteriorates when the molecular weight is lower.

Fig. 16 shows the spinodal curves of the PS/cyclohexane systems. Experimental data are reported by Scholte et al. [39], and critical points are taken from Koningsveld et al. [40]. We still use the same model parameters $M_w/r_2=135.7$ and $\varepsilon/k=87.1$ as in Fig. 15. Similarly, the predicted result for system having longer chain is better than that having shorter chain. Recently, Qiao and Zhao [41] developed a theory; their results (dot lines) are also presented as a comparison. But it should be noted that the chain length is not dependent on the molecular

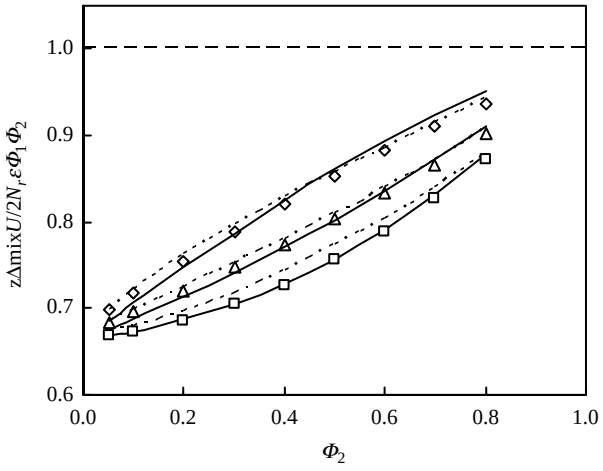

Fig. 11. Normalized internal energy of mixing for a binary lattice polymer solution with $r_2=8$. MC data: $kT/\varepsilon=4$ (open squares); $kT/\varepsilon=10$ (open triangles); $kT/\varepsilon=-10$ (open diamonds). Solid lines: this work. Dot line: Freed theory. Dash line: Flory–Huggins theory.

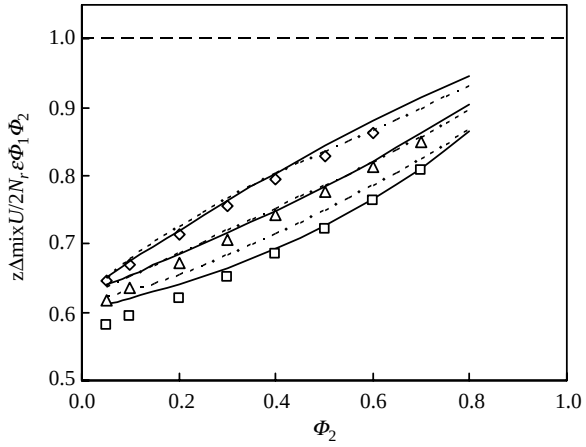

Fig. 12. Normalized internal energy of mixing for a binary lattice polymer solution with $r_2=64$. Legend: the same as Fig. 11.

weight and the energy parameters are also not a constant in their work.

5. Discussion and conclusion

We have developed a molecular thermodynamic model with concise and accurate expressions for the Helmholtz energy of mixing and other thermodynamic properties for binary lattice polymer solutions. It is composed of three terms: the Guggenheim's athermal entropy of mixing, the residual Helmoltz energy of mixing of an Ising lattice, and the contribution of dissociation and association described by the r-particle correlation function. In the latter, a parameter λ characterizing the long-range correlations beyond the close contact pairs is introduced. Besides the pre-factor, the main part of the parameter λ is linearly chain-length dependent. The dependence is determined by simulated critical parameters for two systems with chain lengths of 4 and 200. Tested comprehensively by comparing the predicted critical temperatures and compositions, coexistence curves, spinodals and the internal energies of mixing with the corresponding simulation

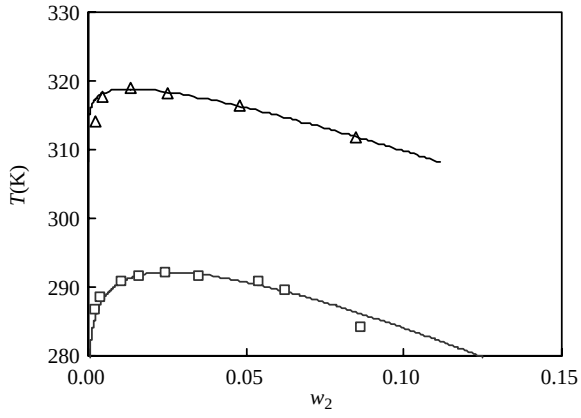

Fig. 13. Coexistence curves of PIB/diisobutyl ketone mixtures. Experimental data [36]: $M_w=22{,}700$ (squares); $M_w=285{,}000$ (triangles). Solid lines: this work, $r_2=520$, $\varepsilon/k=87.2$ K, $M_w=22{,}700$; $r_2=4500$, $\varepsilon/k=92.1$ K, $M_w=285{,}000$.

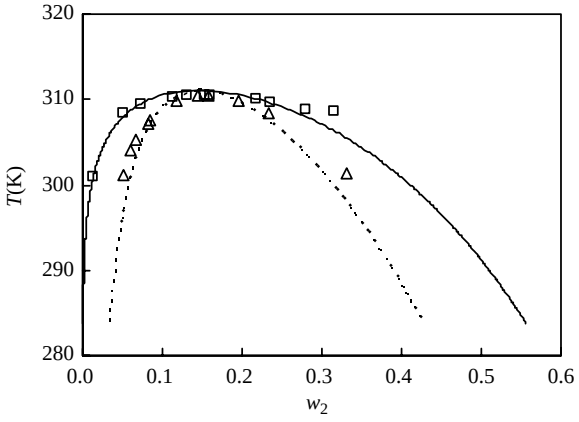

Fig. 14. Binodal and spinodal curves of polystyrene (PS)/methyl cyclohexane mixture. Experimental data [37]: binodal curve (squares); spinodal curve (triangles). Solid lines: this work, $r_2 = 270$, $\varepsilon/k = 94.7$ K.

results and experimental data for different systems covering a wide range of chain lengths indicating the reliability and feasibility of the model developed and the characteristic parameter introduced. The results also indicate the superiority of the model over other theories including the rigorous Freed theory. For practical applications, preliminary examples show good behavior except for cases with shorter chains. The model can serve as a basis to develop more efficient models, for example, constructing a double-lattice model [16–19] to account for the orientation effect of hydrogen bonding, therefore, more complex phase behavior such as LCST, loop and hour-glass type coexistence curves can be accurately described.

In developing a theoretical model, statistical mechanics is generally a first choice. However, its power is always limited because of the mathematical difficulties. Molecular thermodynamics seeks to overcome this limitation. Besides some semi-empirical approach based on concepts from statistical mechanics, on ideas from molecular physics and on information from molecular structures, introducing molecular simulation results to overcome the mathematical difficulties gives us new impetus to develop more accurate models. The

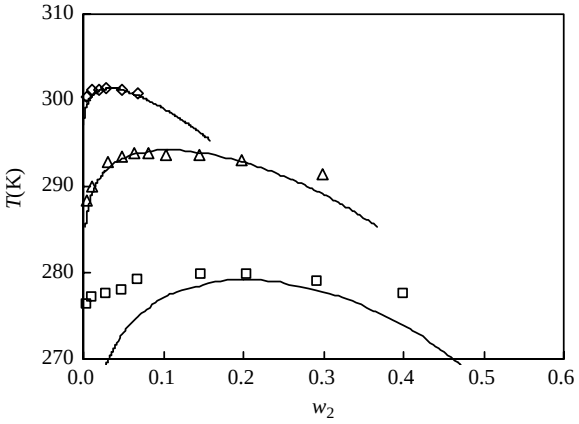

Fig. 15. Coexistence curves of PS/cyclohexane mixtures. Experimental data [38]: $M_w = 20{,}400$ (squares); $M_w = 100{,}000$ (triangles); $M_w = 610{,}000$ (diamonds). Solid lines: this work.

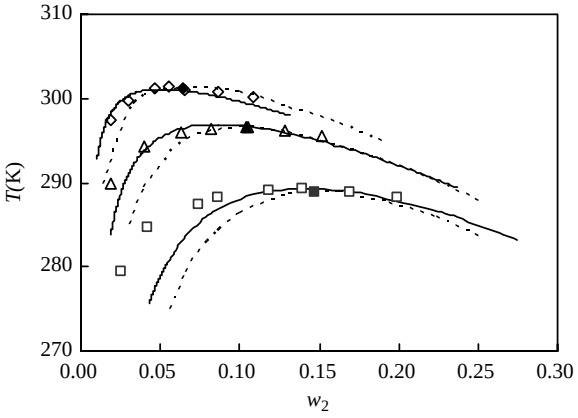

Fig. 16. Spinodal curves of PS/cyclohexane systems. Experimental [39]: $M_w = 51{,}000$ (squares); $M_w = 163{,}000$ (triangles); $M_w = 520{,}000$ (diamonds). Corresponding critical points from Koningsveld et al. [40]. Solid lines: this model. Dot lines: Qiao and Zhao's theory [41].

method used in this work retains the rigorous of the statistical mechanics. At first, analytical expression is obtained, however, it may contain unknown functions or coefficients because of the mathematical difficulty or sometimes because of the simplification introduced. The form of the unknown functions or unknown coefficients is then determined by a few computer-simulation results. This work proves that this method is very effective as shown by the final concise expressions and the good quality of the predictions. The key of using this method to meet with success lies in the reasonable choice of the form of the unknown function and the high quality of simulation results. In this respect, there is still room for improvement on the term characterizing the long-range correlations of this work.

Acknowledgements

This work was supported by the National Natural Science Foundation of China (20236010, 20476025, 20490200), the Doctoral Research Foundation sponsored by the Ministry of Education of China (Project No. 20050251004), E-institute of Shanghai High Institution Grid (No. 200303), Shanghai Municipal Science and Technology Commission of China (No. 05DJ14002) and Shanghai Municipal Education Commission of China.

References

[1] Flory PJ. J Chem Phys 1941;9:660–1. Flory PJ. J Chem Phys 1942;10:51–61. Flory PJ. J Am Chem Soc 1965;87:1833.
[2] Huggins ML. J Chem Phys 1941;9:440. Huggins ML. J Phys Chem 1942;46:151–8.
[3] Fisher ME. Rep Prog Phys 1967;30:615.
[4] Heller P. Rep Prog Phys 1967;30:731.
[5] Sengers JV, Sengers JM. In: Croxton CA, editor. Progress in liquid physica. New York: Willey; 1978 [chapter 4].
[6] Guggenheim EA. Mixtures. Oxford: Oxford University Press; 1952.
[7] Koningsveld R, Kleintjens LA. Macromolecules 1971;4:637–41.
[8] Freed KF. J Phys A: Math Gen 1985;18:871–87.
[9] Pesci AI, Freed KF. J Chem Phys 1989;90:2017–26.
[10] Madden WG, Pesci AI, Freed KF. Macromolecules 1990;23:1181–91.

[11] Dudowicz J, Freed KF. Macromolecules 1990;23:1519–26. Dudowicz J, Freed KF. Macromolecules 1991;24:5076–95 [see also p. 5096–111 and 5112–23].
[12] Dudowicz J, Freed KF, Madden WG. Macromolecules 1990;23:4803–19.
[13] Dudowicz J, Freed KF. Theo Chim Acta 1992;82:357–82.
[14] Yan Q, Liu H, Hu Y. Macromolecules 1996;29:4066–71.
[15] Panagiotopoulos AZ, Wong V. Macromolecules 1998;31:912–8.
[16] Hu Y, Lambert SM, Soane DS, Prausnitz JM. Macromolecules 1991;24:4356–63.
[17] Hu Y, Liu H, Soane DS, Prausnitz JM. Fluid Phase Equilibria 1991;67:65–86.
[18] Hu Y, Liu H, Wu D, Prausnitz JM. Fluid Phase Equilibria 1993;83:289–300.
[19] Hu Y, Liu H, Shi Y. Fluid Phase Equilibria 1996;117:100–6.
[20] Lambert SM, Soane DS, Prausnitz JM. Fluid Phase Equilibria 1993;83:59–68.
[21] Chang BH, Ryu KO, Rae YC. Polymer 1998;39:1735–9.
[22] Chen T, Liu H, Hu Y. Macromolecules 2000;33:1904–9.
[23] Chen T, Peng C, Liu H, Hu Y. Fluid Phase Equilibria 2005;233:73–80.
[24] Chang BH, Bae YC. Chem Eng Sci 2003;58:2931–6. Chang BH, Bae YC. J Polym Sci, Part B: Polym Phys 2004;42:1532–8.
[25] Hill TL. Statistical mechanics. Maiderherd: McGraw-Hill; 1956.
[26] Carnahan NF, Starling KE. J Chem Phys 1969;51:635–6.
[27] Hu Y, Liu H, Prausnitz JM. J Chem Phys 1996;104:396–404.
[28] Cummings PT, Stell G. Mol Phys 1985;51:25 [see also p. 33–48].
[29] Stell G, Zhou YQ. J Chem Phys 1989;91:3618–23.
[30] Zhou YQ, Stell GJ. Chem Phys 1992;96:1504–6 [see also p. 1507–15].
[31] Tildesley DJ, Streett WB. Mol Phys 1980;41:85–94.
[32] Yan Q, Liu H, Hu Y. Fluid Phase Equilibria 2004;218:157–61.
[33] Widom B. J Chem Phys 1963;39:2808–12.
[34] Rodriguez AL, Freire J, Horta A. J Phys Chem 1992;96:3954–8.
[35] Siepman JI, Frenkel D. Mol Phys 1992;75:59–70.
[36] Flory PJ, Shultz AR. J Am Chem Soc 1952;74:4760–7.
[37] Rong ZM, Wang HQ, Ying XG, Hu Y. J East China Univ Sci Technol (Chin) 1996;22:754–9.
[38] Bae YC, Lambert SM, Soane DS, Prausnitz JM. Macromolecules 1991;24:4403–7.
[39] Scholte TG. J Polym Sci, Part A-2 1971;9:1553–77.
[40] Koningsveld R, Kleintjens LA, Schultz AR. J Polym Sci, Part A-2 1970;8:1261–78.
[41] Qiao B, Zhao D. J Chem Phys 2004;121:4968–73.